

Fluorescence Study of the Core/Shell Interface in Polyelectrolyte Micelles. Binding of Fluorescent Surfactants in the Interfacial Region

Kateřina Krijtov,¹ Miroslav Štepnek,¹ Karel Prochzka,^{1,3} and Stephen E. Webber²

Received July 14, 1997; accepted January 14, 1998

Properties of the interfacial region between the nonpolar core and the polar shell in polystyrene-*block*-poly(methacrylic acid) micelles were studied by fluorescence techniques using 5-(*N*-octadecanoyl) aminofluorescein (OAF) as a probe for microfluidity and local pH. The block copolymer used was tagged between blocks by one 9,10-diphenylanthracene (DPA) group, which allowed us to study binding of OAF at the interface by means of nonradiative energy transfer between DPA and OAF. A shift in the pK_a of OAF and appreciable changes in anisotropy and quenching efficiency due to immobilization of the fluorophore head-group in hydrophobic poly(methacrylic acid) domains were observed after binding of the probe at the interface.

KEY WORDS: Core/shell interface; polyelectrolyte micelles; binding; fluorescent surfactants.

INTRODUCTION

Amphiphilic block copolymers consisting of a long nonpolar block and a long polyelectrolyte block (either a strong or a weak polyelectrolyte) are able to form multimolecular micelles with compact nonpolar cores and polyelectrolyte brush-like shells in aqueous buffers [1]. Block copolymers containing a long and strongly hydrophilic block are insoluble in water and polyelectrolyte micelles have to be prepared indirectly, e.g., by stepwise dialysis from water-organic solvent mixtures into a purely aqueous solvent [2]. Hydrophobic cores of micelles are in a kinetically frozen nonequilibrium state in aqueous media [2] and the properties of micellar solutions depend strongly on the dissociation degree of polyelectrolyte groups in the shell [3]. The dissociation

degree does not correspond to the bulk pH. It is suppressed in the inner part of the shell and increases toward the periphery of the micelle [4].

Amphiphilic fluorophores, such as 5-(*N*-octadecanoyl)aminofluorescein (OAF) and 4-heptadecyl-7-hydroxycoumarin, bind at amphiphilic interfaces and may be used as probes for studies of interfacial micropolarity, microfluidity, and local pH. It has been shown by Fernandez and Fromherz [5] that their behavior at the interfaces is influenced by changes in the microenvironment polarity and by the presence of the electric double layer. Both phenomena affect dissociation of polyelectrolyte groups (they cause a shift in the pK_a value) and, consequently, fluorescence properties of the fluorophore.

In this study, OAF was used to probe the local pH and microfluidity of the interfacial region of polystyrene-*block*-poly(methacrylic acid) (PS-PMA) micelles in aqueous buffers in the pH range from 5 to 10. The copolymer used was tagged between blocks by a 9,10-diphenylanthracene (DPA) group. When polymeric micelles are formed in aqueous media, all DPA groups are localized at the core/shell interface. Therefore meas-

¹ Department of Physical and Macromolecular Chemistry, Faculty of Science, Charles University in Prague, Albertov 2030, 128 40 Prague 2, Czech Republic.

² Department of Chemistry and Biochemistry and Center for Polymer Research, University of Texas at Austin, Austin, Texas 78712.

³ To whom correspondence should be addressed.

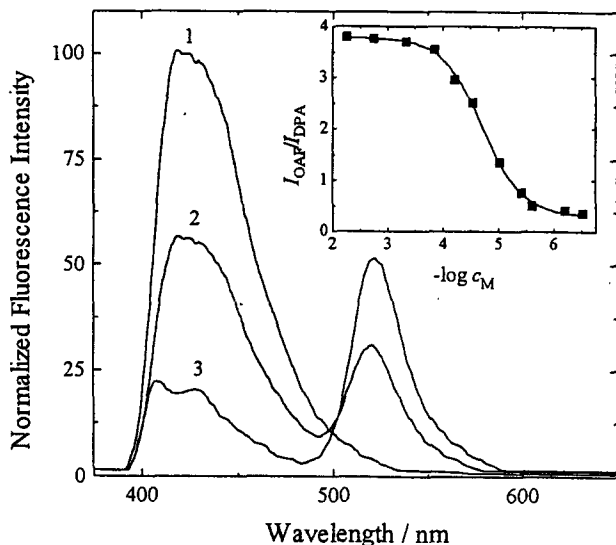


Fig. 1. Emission spectra of DPA-tagged micelles (excitation, 359 nm): 1, without OAF; 2, with 1.6×10^{-6} M OAF; 3, with 4.2×10^{-6} M OAF. Inset: OAF-to-DPA fluorescence intensity ratio vs. concentration of micelles; c_M in $\text{g}\cdot\text{ml}^{-1}$ (OAF—emission, 520 nm; DPA—emission, 411 nm; excitation, 359 nm).

measurements of nonradiative energy transfer (NRET from DPA to OAF) monitor OAF penetration into the inner part of the shell. Supplementary information on the bound OAF is obtained from OAF steady-state fluorescence anisotropy and fluorescence quenching by Ti^+ cations.

EXPERIMENTAL

OAF was purchased from Molecular Probes. DPA-tagged polystyrene-*block*-poly(methacrylic acid) was prepared as described elsewhere [6]. Weight-averaged molar mass, polydispersity, and mass fraction of the polystyrene block were 5.7×10^4 , 1.05, and 0.4, respectively. Other chemicals were purchased from Aldrich.

Micelles were prepared by stepwise dialysis of the copolymer solution in 1,4-dioxane–aqueous buffer mixture with 80% 1,4-dioxane against solutions with decreasing amounts of 1,4-dioxane and, finally, against pure buffer. For the pH range from 5.0 to 9.0, sodium phosphate and tetraborate buffers were used; higher pH's were achieved by the addition of NaOH. Ionic strength of all buffers was 0.15. Final concentration of the copolymer was ca. 2×10^{-3} $\text{g}\cdot\text{ml}^{-1}$. Apparent molar mass and hydrodynamic radius of the micelles were 8×10^6 and 35 nm, respectively [6].

Steady-state measurements were performed with a Fluorog 2 fluorometer (SPEX, USA). Time-resolved measurements were carried out with an ED 299/T fluorometer (Edinburgh Instruments, Great Britain). Quasi-elastic light-scattering measurements of the hydrodynamic radius of micelles were performed using a Brookhaven 2030 instrument [8].

RESULTS AND DISCUSSION

Multimolecular polyelectrolyte PS-PMA micelles in neutral and alkaline buffers contain compact spherical cores of radius $R_c = 12$ nm formed by PS blocks [7] and water-soluble shells formed by partially charged PMA blocks. The hydrodynamic radius of micelles in the alkaline solution (pH 9, $I = 0.15$) is $R_H = 35$ nm. Due to the fact that all PS-PMA chains are tagged between blocks by one pending DPA group per chain, all DPA tags in multimolecular micelles are localized close to the core/shell interface. Since there exists a strong overlap in the DPA emission spectrum and the fluorescein absorption spectrum [8], NRET measurement is a suitable technique for studying the binding of OAF at the core/shell interface. Together with the microenvironment-sensitive fluorescence of OAF, it allows for two independent types of fluorescence measurements.

(a) Nonradiative energy transfer from DPA to OAF was used to prove that OAF binds strongly at the core/shell interface of PMA micelles. Figure 1 shows the fluorescence of DPA (excitation at 359 nm, emission about 410 nm) and the sensitized fluorescence of the micelle-bound OAF at about 520 nm (OAF fluorescence provoked by the excitation at 359 nm is negligible). Curve 1 is the emission spectrum of micelles ($c_M = 2 \times 10^{-3}$ $\text{g}\cdot\text{ml}^{-1}$) without the addition of OAF. Curves 2 and 3 correspond to the OAF concentrations, $c_{\text{OAF}} = 1.6 \times 10^{-6}$ and 4.2×10^{-6} M, respectively. A decrease in the DPA emission band and the appearance of the OAF emission indicate an efficient NRET. The same conclusion may be drawn from the time-resolved measurement of the DPA emission (Fig. 2), which shows a decrease in the fluorescence lifetime of the donor with increasing concentrations of the acceptor. A more detailed study and analysis of energy transfer data exceed the scope of this paper and will be published later.

A stepwise dilution of the solution containing a constant mass ratio of DPA-tagged micelles and OAF by the solvent and measurement of the ratio of acceptor-to-donor emission, $I_{\text{OAF}}/I_{\text{DPA}}$, as a function of the concentration of micelles allows us to estimate an approximate value of the partition coefficient, K_p , of

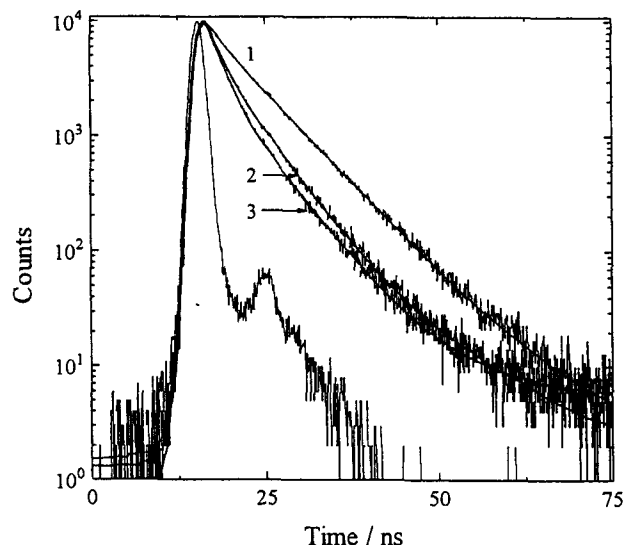


Fig. 2. Time-resolved fluorescence from DPA-tagged micelles (excitation, 359 nm; emission, 411 nm): 1, without OAF; 2, with 1.6×10^{-6} M OAF; 3, with 4.2×10^{-6} M OAF.

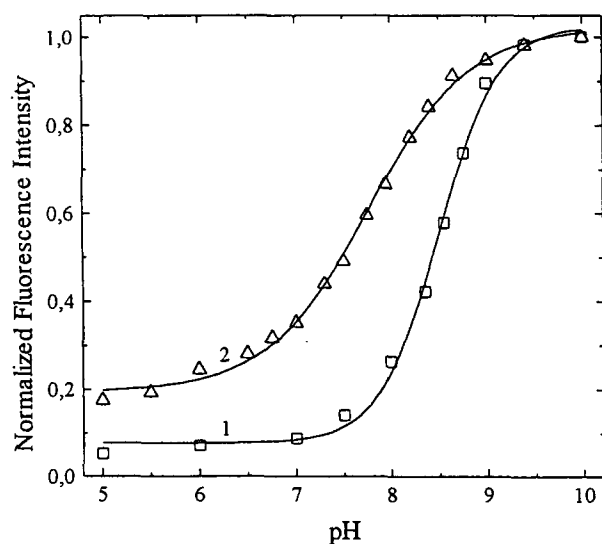


Fig. 3. Fluorescence intensity vs. bulk pH (excitation, 496 nm; emission, 520 nm): 1, free OAF; 2, OAF bound at the micelles.

OAF between micelles and the aqueous phase. This evaluation yields only the first estimate of K_f since NRET between two probes depends on the sixth power of the reciprocal distance between fluorophores and the measured value is not directly proportional to the concentration of the bound OAF. The plot of $I_{\text{OAF}}/I_{\text{DPA}}$ vs $\log c_M$ is shown in the insert in Fig. 1 for the initial micellar concentration, $c_M = 2 \times 10^{-3}$ g·ml $^{-1}$, and the concentration of OAF, $c_{\text{OAF}} = 10^{-6}$ M. The shape of the

curve allows for unambiguous evaluation of the order of magnitude of K_f , ca. 10^5 . This value suggests that the binding is fairly strong since K_f is comparable with partition coefficients for very nonpolar molecules in aqueous solutions of PS-PMA micelles (such as pyrene [2]).

(b) The second type of measurements is based on the microenvironment-sensitive fluorescent properties of OAF only. Dissociation of the -OH group in the hydrophilic head-group of the interface-bound amphiphilic fluorescein-based surfactants depends on the polarity and charge of the core/shell interface and the fraction of fluorescently active dianions in the studied system changes compared with that in the bulk solution. However, the fluorescence behavior of fluorescein-based probes with long nonpolar chains differs from that of short-chain probes in several aspects. In contrast to short-chain probes, the fluorescence intensity of OAF increases strongly after its binding at the core/shell interface of PS-PMA micelles in a broad pH region, ranging from 4 to 11.

The normalized fluorescence intensities, I_F , vs the pH for the free OAF (curve 1) and the micelle-bound OAF (curve 2) are shown in Fig. 3. Both emission intensities were measured at 520 nm for direct excitation of the probe at 496 nm. They are normalized by corresponding limiting intensities in strongly alkaline solutions (pH 11). The absolute intensity (per unit concentration) of the free probe is ca. 10^2 times weaker than that of the micelle-bound probe and the former depends strongly on I .

The enormous increase in the emission intensity (which is evident also at high pH's) and the change of the curve shape after OAF binding are slightly surprising. The sigmoidal part of the curve is shifted in the direction opposite to the theoretical expectation [5], and the slope is appreciably less steep. This behavior may be understood on the basis of the following observations.

(i) The solubility of OAF in aqueous solutions is very low due to the hydrophobicity of the long aliphatic chain. Surfactants with hydrocarbon chains longer than 12 (-CH $_2$ -) units are known to form dimers, or small oligomers at very low concentrations, i.e., at concentrations that are one or two orders of magnitudes lower than the c.m.c. [9]. Fluorescence in OAF oligomers is self-quenched, similarly to the fluorescein self-quenching at higher concentrations. Since the concentration of the PS-PMA copolymer in our experiments is relatively high (2×10^{-3} g·ml $^{-1}$) compared with the fluorophore concentration, which is only 10^{-6} M, the OAF molecules bind at the core/shell interface as monomers. The bound probes are on average far away from each other, which prevents self-quenching, and the fluorescence intensity increases strongly in the whole pH region.

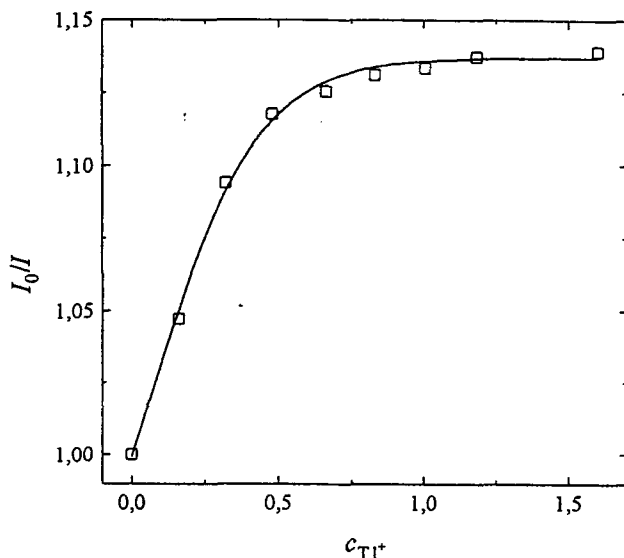


Fig. 4. Stern-Volmer plot for quenching of fluorescence of OAF bound at the micelles by Tl^+ ; c_{Tl^+} in $10^{-2} \text{ mol} \cdot \text{l}^{-1}$.

(ii) After binding at the interface, the aliphatic tail of the OAF is buried in the nonpolar core, and the hydrophilic fluorescein group is localized in the inner part of the shell close to the interface. Dissociation of carboxylic groups is suppressed close to the core [4] and PMA forms a very hydrophobic and relatively compact inner layer of the shell. This behavior is similar to the formation of hydrophobic domains in dilute solutions of linear PMA at a low pH [10], however, the compactness and hydrophobicity of the inner part of the shell are expected to be more pronounced compared with hydrophobic domains in linear PMA due to the significantly high local PMA concentration close to the core/shell interface.

The assumption that the fluorescein head-group of the bound OAF is trapped and immobilized in the compact and hydrophobic microenvironment is supported by fluorescence anisotropy and quenching measurements. Steady-state anisotropy, $\langle r \rangle$ (excitation at 496 nm, emission at 520 nm), was measured as a function of pH. Measured values are fairly high and decrease with increasing pH (e.g., $\langle r \rangle = 0.30, 0.23,$ and 0.15 for pH 6, 7, and 9, respectively). Since the fluorescence lifetimes are almost-constant in the studied region of pH (τ_F ca. 4.5 ns), the steady-state anisotropy monitors the local mobility of the probe fairly well. An increase in the probe mobility with increasing pH corresponds to the general knowledge of the behavior of polyelectrolyte shells in water-soluble micelles. Increasing pH promotes dissociation of carboxylic groups and stretch-

ing of PMA blocks in the shell. The local concentration of PMA decreases significantly in the outer layer of the shell and slightly in the inner layer. The compactness of the inner hydrophobic layer therefore decreases with rising pH.

A similar conclusion may be drawn from quenching experiments. Fluorescence of the micelle-bound OAF is virtually unquenchable by Tl^+ at low pH's despite the fact that the shell is formed by anionic PMA and the electrostatic attractive force should facilitate the penetration of Tl^+ into the shell. At a high pH, little quenching has been observed. The Stern-Volmer plot is shown in Fig. 4. The nonlinearity and the pronounced down-curvature of the plot together with the low I_0/I value at the saturation limit indicate a very low fraction of probes that may be quenched by thallium. We assume that a small fraction of dissolved OAF molecules that are in equilibrium with the bound OAF may be quenched in the bulk solution. Their contribution to the measured fluorescence is more significant and quenching is more evident at high pH's. This assumption is supported by quenching of the sensitized fluorescence, which is very inefficient in the whole pH region. Study of this problem is in progress and results will be reported soon.

With increasing pH, a significant dissociation of $-COOH$ groups occurs in the middle and outer parts of the shell. This dissociation is accompanied by much less pronounced dissociation in the inner part of the shell. Since the probe monitors the behavior of its close microenvironment, the slope of the sigmoidal part of the fluorescence intensity-vs.-pH curve is less steep in micelles than that in the bulk solution. The micellar shell is broad and its properties (density, degree of dissociation, micropolarity, etc.) change continuously. There is nothing like the electric double layer at the interface which would hinder the escape of protons into the bulk solution similarly to the case of the anionic surfactant micelles. The dissociation of a certain smaller fraction of proton-generating groups (i.e., carboxylic groups in PMA blocks and, also, phenolic groups in OAF) in the inner layer is in fact driven by dissociation processes in the shell to compensate for the overall loss of protons in the middle part of the shell during the rise in pH. This effect decreases the effective pK_a of the OAF.

ACKNOWLEDGMENTS

This work was supported by Grants 203/97/0249 (Grant Agency of the Czech Republic) and 1197/1997 (Grant Agency of Charles University).

REFERENCES

1. (a) D. Kiserow, K. Procházka, C. Ramireddy, Z. Tuzar, P. Munk, and S. E. Webber (1992) *Macromolecules* **25**, 461. (b) K. Procházka, T. J. Martin, P. Munk, and S. E. Webber (1996) *Macromolecules* **29**, 6518.
2. T. Cao, P. Munk, C. Ramireddy, Z. Tuzar, and S. E. Webber (1991) *Macromolecules* **24**, 6300.
3. M. A. Karymov, K. Procházka, J. M. Mendenhall, T. J. Martin, P. Munk, and S. E. Webber (1996) *Langmuir* **12**, 4748.
4. E. B. Zhulina, T. M. Birsthein, and O. V. Borisov (1995) *Macromolecules* **28**, 1491.
5. M. S. Fernández and P. Fromherz (1977) *J. Phys. Chem.* **81**, 1755.
6. A. R. Eckert, T. J. Martin, and S. E. Webber (1997) *J. Phys. Chem. A* **101**, 1646.
7. J. Pleštil, K. Procházka, G. Wignall, Y. Melnicenko, and S. E. Webber, Unpublished data
8. I. B. Berlman (1971) *Handbook of Fluorescence Spectra of Aromatic Molecules*, Academic Press, New York.
9. P. Mukerjee (1965) *J. Phys. Chem.* **69**, 2821.
10. B. Bednář, J. Trněná, P. Svoboda, Š. Vajda, V. Fidler and K. Procházka (1991) *Macromolecules* **24**, 2054.